Environmental Pollution
January 2024, Volume 340 Issue Part 2 Pages 122785 (10p.)
https://doi.org/10.1016/j.envpol.2023.122785
https://archimer.ifremer.fr/doc/00858/97020/

Copper isotopes as a tool to trace contamination in mangroves from an urbanized watershed

Barreira João [1, *], Ferreira Araujo Daniel [2], Rodrigues Breno Q.A. [1], Tonhá Myller [3], De Araújo Rafael [2], Souto-Oliveira Carlos Eduardo [4], Babinski Marly [4], Knoery Joël [2], Sanders Christian J. [5], Garnier Jérémie [3], Machado Wilson [1]

[1] Geochemistry Program, Chemistry Institute, Fluminense Federal University, Brazil
[2] Ifremer, CCEM Contamination Chimique des Ecosystèmes Marins, F-44000, Nantes, France
[3] Geosciences Institute, University of Brasília, Brazil
[4] Geosciences Institute, University of São Paulo, Brazil
[5] National Marine Science Center, Southern Cross University, Australia

* Corresponding author : João Barreira, email address : joao_barreira@id.uff.br

Abstract :

This study investigates the chronology of copper (Cu) contamination and its stable isotopes within an emblematic Brazilian mangrove impacted by multiple urban and industrial Cu sources, deforestation, and eutrophication. In particular, it tests Cu isotopes as tracers of anthropogenic inputs into an anthropized watershed impacted by multiple sources. To do so, we used multi-isotopic approaches (δ65Cu, δ13C, and δ15N), elemental analyses (Al, Ca, Fe, P, Cu, C, and N), and selective and sequential extractions in a210Pb-dated sediment core. This geochemical "toolbox" allowed identifying two main stages of Cu evolution in the sediment core. In the first stage, before 1965, Cu isotope fingerprints responded to landscape changes, indicating a shift from marine to geogenic dominance due to the remobilization and erosion of terrestrial materials. In the second stage, after 1965, the sediment geochemical profile showed increased Cu total concentrations with a higher bioavailability (as reflected by sequential extraction data) accompanying changes in Cu isotope signatures towards anthropogenic values. The findings evidence that local industrial sources, possibly combined with diffuse urban sources, export Cu into downstream mangroves with a distinguishable isotope signature compared to natural values. This study demonstrates the applicability of Cu isotopes as new environmental forensic tools to trace anthropogenic sources in mangrove sediments. Incorporated into a robust geochemical toolbox that combines inorganic and organic proxies for sedimentary materials, this new tool provides a comprehensive understanding of Cu dynamics in mangrove ecosystems, shedding light on the historical and current sources of Cu.

Graphical abstract

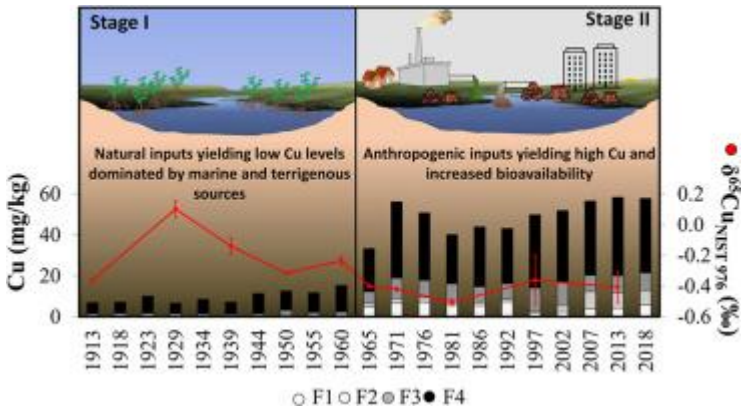

Highlights

► Chronological survey of a well-constrained Brazilian mangrove core. ► Cu isotopes respond to shifts from marine to geogenic dominance. ► Sediments record the evolution of Cu fluxes along periods of urban and industrial development. ► Mangrove sediments record anthropogenic Cu isotope fingerprint. ► Anthropogenic inputs yielding increased bioavailability of Cu in mangrove sediments.

Keywords : isotope source tracking, isotope tracer, marine pollution, anthropogenic Cu, Cu solid partition, metal source, metal fate

1. Introduction

Mangrove sediments effectively trap and accumulate particle-reactive pollutants that are often persistent (Machado et al., 2002a, 2002b; Defew et al., 2005; Tang et al., 2022). Furthermore, anthropogenic forcing can turn such pollutant traps into secondary, legacy sources of contaminants that can affect their surrounding areas and food webs (Harbison, 1986; Bastakoti et al., 2019; Lacerda et al., 2022; Queiroz et al., 2022; Tang et al., 2022). As a result, it is worthwhile to develop tools that can discriminate the status of mangrove sediments either as sources or traps of contamination in their surrounding environments.

In theory, tracking the stable isotopes of any given trace metal that are unevenly distributed in the critical zone offers a potential solution to this issue, since they can provide information on the cycling of their parent element (Albarède, 2004; Komárek, et al., 2008; Weiss et al., 2008; Wiederhold, 2015; Zhong et al., 2020). Previous studies have shown that trace metal isotopes can effectively quantify sources of contamination in mangrove sediments impacted by a single primary source (Araújo et al., 2017, 2018; Tonhá et al., 2020; Jeong et al., 2023a). However, there is currently no record of the use of trace metal stable isotopes in mangrove sediments affected by multiple anthropogenic sources, which is a common scenario in coastal regions with diverse and changing land uses.

Previous studies have successfully used Cu isotopes to assess source apportionment and characterize the combined influences of sources and biogeochemical processes (Petit et al., 2008; Thapalia et al., 2010; El Azzi et al., 2013; Petit et al., 2013; Briant et al., 2016; Araújo et al., 2019b; Briant et al., 2022; Jeong et al., 2023a,b). Thapalia et al. (2010) are perhaps the only ones using Cu isotopes as chronological anthropogenic source tracers. There is a limited number of studies that evaluated the contribution of Cu isotopic tools in coastal areas (Petit et al., 2008; Vance et al., 2008; Petit et al., 2013; Little et al., 2017; Araújo et al., 2019a,b; Ciscato et al., 2019; Briant et al., 2022; Jeong et al., 2023a,b), and only seven dealt with modern sedimentary samples (Little et al., 2017; Araújo et al., 2019a; Araújo et al., 2019b; Ciscato et al., 2019; Briant et al., 2022; Jeong et al., 2023a,b). Jeong et al. (2023a) identified a single anthropogenic source

(electroplating industry wastes) imprinting particular Cu isotope signature in mangrove sediments.

The application of Cu isotopes in the context of mangrove sediments affected by multiple urban and industrial sources presents certain challenges. First, there is the potential for isotopic fractionation of Cu caused by low-temperature biogeochemical processes (Wang et al., 2021). Second, the geochemical reactivity of sedimentary trace metals in highly productive coastal environments can be elevated due to redox reactions (Clark et al., 1998; Marchand et al., 2006, 2014), leading to significant isotopic fractionation (Huan et al., 2020; 2021), which may overshadow source fingerprints. Finally, isotopic signatures of anthropogenic sources of trace metals can vary widely. In some urban areas it is impractical to assess each anthropogenic source isotopic ratio, making it difficult to differentiate their resulting group from natural sources.

Therefore, when considering mangrove sediments under this scenario, it is helpful to combine Cu isotopes with multiple geochemical analyses to aid in the elucidation of source apportionment, as performed in previous geochemical "toolbox" approaches (He et al., 2020; Tonhá et al., 2020, 2021). Proxies include sequential extractions combined with isotopic data, and furthermore, chronologies of the study area are imperative to validate the use of these proxies for reconstructing the environmental changes controlling the metal pollution history.

Based on these premises, and with the purpose of advancing the current understanding of the role of mangroves in trace metal cycling, we conducted a series of analyses on a sediment core extracted from a mangrove in the Estrela River basin in Rio de Janeiro, Brazil. The study area is subject to various environmental stressors, including mangrove deforestation (Borges et al., 2006, 2009), high levels of metal contamination (Rebello et al., 1986; Leal & Rebello, 1993; Rangel et al., 2011), and nutrient inputs that lead to eutrophication in most parts of the bay (Soares-Gomes et al., 2016; Fries et al., 2019). The core was dated using ^{210}Pb and subjected to various analyses including multi-isotopic (δ^{65}Cu, δ^{13}C, δ^{15}N), elemental (Al, Ca, Fe, P, Cu, C and N), and partial extractions (BCR method; Tonhá et al., 2020; Rauret et al., 1999). The primary aim of the present study was to reconstruct historical changes on geochemical compositions of mangrove sediments influenced by urban and industrial development while also assessing the suitability of Cu isotopes for use in this context.

2. Materials and methods

2.1. Study Area

Figure 1 shows the sampling point in Guanabara Bay, Rio de Janeiro, Brazil and its surrounding land use. The study area is bordered to the north by an urban agglomeration and to the south by the Guanabara Bay. Deforestation around 1980 is witnessed by residents and revealed by remote sensing data (Borges et al., 2009, 2006).

The sampling point is situated in the Estrela River basin, which discharges into the northwest section of Guanabara Bay. The river separates the southern part of the cities of Magé (to the east) and Duque de Caxias (to the west). The middle part of the hydrographic basin and some lower areas have been highly urbanized, and half of the sewage is untreated before discharging (SNIS, 2020). Unsurprisingly, the sampling location has the second lowest water quality rating in the Bay (Kjerfve et al., 1997; Fries et al., 2019).

The industrialization of the Estrela River hydrographic basin dates back to the 1830s when the Gunpowder Factory, now known as the Brazilian War Material Industry (IMBEL), began operations (AN, 2016). Since then, numerous other industries have been established in the region.

Previous studies reported varying Cu concentrations in sediments from the Estrela River bed. Rebello et al. (1986) found a high concentration of Cu (up to 2,112 mg/kg), while Rangel et al. (2011) found a maximum Cu concentration of 74.5 mg/kg.

Two significant historical events from the 20th century have a highlighted potential of impacting mangrove sediments in the watershed. The first event was the road's opening connecting the cities of Rio and Petrópolis in 1928, which marked a step in the regional economic development (AGEVAP, 2021). The second event was the period of intense industrialization and population growth in the 1960s, corresponding to the worsening of the environmental problem in the Guanabara Bay (Alencar, 1980; Godoy et al., 1998; Monteiro et al., 2012). This unplanned urban development resulted in mangrove deforestation for land reclamation, as observed in the study area.

2.2. Sampling and samples preparation

Sediment samples were collected from a mangrove area at the estuary of the Estrela River using a Cu-clean polyethylene tube. A sedimentary core of 41 cm (-22.7203°N and -43.1961°E) was obtained, and sectioned at 2 cm intervals, with each slice constituting a

sample. The sediment samples were then lyophilized, disaggregated, and homogenized by grinding with agate mortar and pestle.

A portion of the samples was sieved eliminate the sand (>63µm) fraction, for the analysis of total composition of elements including Al, Ca, Fe, P and Cu, and for the study of solid partition using the BCR procedure, and Cu isotopic composition. Sieving aimed to remove larger particles and debris that may affect the accuracy of the results. Non-sieved sediment samples were analyzed for total organic C, $\delta^{13}C$, total N, $\delta^{15}N$, granulometry, apparent density, and ^{210}Pb.

2.3. Cleaning procedures

All glassware used for sample preparation underwent a 24-hour immersion in 10% HCl (v/v) and was then rinsed with Milli-Q® water, which was purified through the Milli-Q® purification system (18.2 M.Ohm.cm). Plastic materials used were previously decontaminated with 3% HNO3 (v/v) and rinsed with Milli-Q® water. Savillex® digestion plasticware (PFA) were washed with detergent and Milli-Q® water, decontaminated in a 50% HNO_3 solution (v/v) by boiling for 1 hour. The bottles were then rinsed and the previous step was repeated, followed by triple rinsing in Milli-Q® water.

Resins used for chromatographic separation were washed with Milli-Q® water, left to stand for one night, then washed with 0.5 M HNO_3 and left to stand again for one night. This cycle was repeated three times. Finally, the resin was stored in 0.1M HNO_3 before use.

2.4. Analytical Procedures

2.4.1. Physical characterization: granulometry and dry bulk density

Sediments were analyzed for their granulometry using a CILAS 1064 laser granulometer. The size fractions were measured from 0.04 to 500 µm by diffraction, and the data generated were analyzed using GRADISTAT, a package for grain size distribution and statistics. The apparent densities of the sediments were measured to calculate the sediment and Cu flux, and were obtained by dividing the dry weight of the samples by their wet volume:

$$\rho = \frac{weight_{dry}}{total\ volume} \quad \text{(Eq. 1)}$$

Lyophilization (vacuum drying) was used to dry the samples prior to density measurement.

2.4.2. Organic matter quality and eutrophication indicators: C, $\delta^{13}C$, N and $\delta^{15}N$

The samples were analyzed for organic matter quality and eutrophication indicators, including organic C, $\delta^{13}C$, total N, and $\delta^{15}N$, using a Flash Elemental Analyzer coupled to an IRMS Delta V from Thermo Fisher (Thermo Flash EA 1112). Prior to the analysis of sedimentary organic carbon (C), the samples were decarbonated by adding 1M HCl.

2.4.3. Total and partial digestion and elemental analysis

Total digestion of about 100 mg dry sediment aliquots were performed in Teflon Savillex© vials heated on a coated graphite block using multiple-step acid concentrated procedure with HF, HCl and HNO_3. Blanks and certified reference materials (CRM BHVO-1 and MESS-4) were joined to batch samples. Once completed digestion, acid extracts were transferred to Falcon® tubes and diluted to 50 ml with high-purity water. Aliquots of the final extract were split for subsequent analysis of concentrations and isotopes.

Total concentrations of Cu, Ca, Al, Fe and P were determined using ICP-OES (Spectrometry of Optical Emission by Inductively Coupled Plasma) at Geoquímica Laboratory at University of Brasília. The measured values were always within 10% of the certified values of the CRM BHVO-1 for considered elements. The solid partition of Cu was evaluated using sequential extractions following the modified BCR extraction procedure proposed by Tonhá et al. (2020) based on the original protocol from Rauret et al. (1999) (Supplementary Material). This procedure allows the quantification of elements in four fractions: F1, the exchangeable and carbonate fraction of sediment particles extracted with 0.11 M acetic acid (HAc); F2, the fraction associated with Fe-Mn oxyhydroxides extracted with a 0.5 M hydroxylamine hydrochloride solution; F3, mainly composed of metals associated with reactive sulfides, authigenic pyrites, and organic

matter, extracted with pure H_2O_2 and a 1 M ammonium acetate solution; and F4, assessed by subtracting the results of the first three extractions from the total concentrations.

The concentrations of the fractions were determined using ICP-OES (Spectrometry of Optical Emission by Inductively Coupled Plasma) at Geoquímica Laboratory at University of Brasília. The internal control of the sequential extraction method, calculated as $F\% = 100 \times (F1 + F2 + F3 + F4)/(\text{total digestion})$, reached values lower than 90 or larger than 110% for unknown samples and reference material (BCR 701). All extractions were performed in three independent replicates, and standard deviation between replicates were lower than ±10%. Analytical blanks were made according to the recommendation of Rauret et al. (1999).

2.4.4. Cu isotope analyses

To prepare samples for isotope analysis, we employed a pre-purification step using an ion exchange chromatography column packed with pre-cleaned BioRad AG MP1 resin to remove matrix interferents following the Souto-Oliveira (2018)'s protocol. Briefly, the resin was cleaned three times with 12 mL of 0.5 mol/L HNO_3 and 8 mL of MilliQ water, and then conditioned with 12 mL of 6 mol/L HCl. Samples were loaded in 1 mL of 7 mol/L HCl. Matrix elements were eluted with 1.5 mL of 7 mol/L HCl, and Cu was eluted with 10 mL of 7 mol/L HCl. This step was repeated again to complete Cu purification. Then, the eluted Cu solutions were evaporated to dryness at 120 °C, and a few drops of concentrated HNO_3 were added to break down any possible residue of organic matter, followed by another evaporation to dryness at 120 °C. Finally, the samples were redissolved in 2 mL of 2% (m/m) HNO_3 for instrument analyses. The total procedural blank of Cu was < 3 ng, which is negligible compared with the total Cu sample used in analysis (~1 μg).

The Cu isotope analyses were performed in the Multi Collector (MC)-ICP-MS Neptune Plus at CPGeo's Lab (University of São Paulo. Samples were introduced into the spectrometer with a microconcentric PFA nebulizer (50 μL/min flow) coupled with a two-step expansion chamber and a quartz torch and assisted by an automatic sampler (CETAC ASX-100). Data was obtained through 40 cycles of a 4 s integration measurements, with instrumental baseline and peak blank corrections for each measure.

The samples run bracketed with our in-house "USP" Cu standard and external normalization and exponential law used for mass bias correction. The in-house "USP"

standard is calibrated against the international isotope reference standard for Cu (NIST/SRM-976). The calibration value of $\delta^{65}Cu_{USP/SRM\text{-}976}$ = 0.17 ± 0.04‰ (2σ, n=15) was used to convert data to the NIST/SRM-976. Thus, final isotope compositions were expressed as follows

$$\delta^{65}\mathrm{Cu}_{\mathrm{NIST/SRM\ 976}}(‰) = \left(\frac{\frac{^{65}Cu}{^{63}Cu_{sample}}}{\frac{^{65}Cu}{^{63}Cu_{\mathrm{NIST\ 976}}}} - 1 \right) * 1000 \quad - 0.17 \qquad \text{(Eq. 2)}$$

The calculated $\delta^{65}Cu_{NIST/SRM\ 976}$ values represent the average and the two standard deviations (2 s) of two or three individual measures run in a single analytical session. The routine precision obtained for individual samples and replicates of reference materials was generally better than ±0.05 ‰. The MESS-4 analysis yielded a value of $\delta^{65}Cu_{NIST/SRM\ 976}$ = -0.05 ± 0.01 (2s, n = 4). This value concurs with that from Sullivan et al. (2020) of $\delta^{65}Cu_{NIST/SRM\ 976}$ = -0.09 ± 0.07‰ (2s).

2.4.5. Enrichment Factors (EF) and flux calculations with ^{210}Pb dating

Enrichment Factor is a geochemical index conceived to reduce dilution effects and thus better estimate anthropogenic contributions.

The minimum Cu concentration detected in the present study (6.61 mg/kg, Table 1, Supplementary Material) is higher than background concentrations for other areas in the Guanabara Bay (2.3 to 2.7±0.8 mg/kg; Monteiro et al., 2012; Machado et al., 2002; Rebello et al., 1986; Godoy et al., 1998), yet similar to that from the Jurujuba Cove (9.0±4.7 mg/kg, Baptista-Neto et al., 2000).

The range of Cu background concentrations in Guanabara Bay vary from 2.3 to 9.0±4.7 mg/kg (Rebello et al., 1986; Godoy et al., 1998; Machado et al., 2002; Monteiro et al., 2012; Baptista-Neto et al., 2000), and the industrial development of the Estrela River basin is earlier that the period covered by the sediment core. Therefore, enrichment factors were determined by normalizing the Cu/Al ratio of the Upper Continental Crust (UCC) (Rudnick and Gao, 2003) as follows:

$$Cu\ EF = \frac{\frac{Cu}{Al}sample}{\frac{Cu}{Al}(UCC\ average)}$$ (Eq. 3)

Al is widely used in EF calculation because it is a conservative element that correlates with sediment particle size. It is a major constituent of fine-grained aluminosilicates, with which the bulk of the trace metals associate in natural sediments (Loring, 1991).

Cu fluxes to the sediments were calculated from the equation below, where ρ is the apparent density and *s* is the sedimentation rate, determined after ^{210}Pb dating.

$$Cu\ flux = Cu_{\ concentration} x\ \rho\ x\ s$$ (Eq. 4)

Sedimentation rates and dating were determined using ^{210}Pb. Excess ^{210}Pb activities are linked to atmospheric deposition and were calculated using the differences between total ^{210}Pb and ^{226}Ra activities (Appleby & Oldfield, 1978). A gamma ray spectrometer equipped with a CANBERRA Ge hyper-pure detector was used to collect data, and the Genie-2000 software was used for interpretation.

2.4.6. Statistical analysis

Pearson correlations were performed to evaluate linear relationships between variables. The confidence degree used was the widely accepted and conventional $p < 0.05$. Principal components analysis (PCA) was performed using the STATISTICA© software package to gain an overview understanding of the various parameters evaluated, and their main controlling factors. To compare the isotope data from the present study with literature values, including the central tendency, dispersion, and potential outliers, we provided histograms with theoretical normal distributions.

3. Results and discussion

3.1. Temporal variation of marine and continental proxies

Table 1 (Supplementary Material) summarizes all data obtained from the sediment sample analyses, while Figure 2 shows the temporal evolution of the main parameters analyzed in the study, along with historical markers. To establish a robust basis for the further interpretation of Cu parameters, the vertical distributions of Ca/Al, C/N, δ^{13}C, and δ^{15}N were evaluated beforehand. Ca/Al values were used to access the proportions of

marine $CaCO_3$ and terrestrial materials in the form of Al oxides. The ratio of C/N, $\delta^{13}C$, and $\delta^{15}N$ assist in interpreting the relative contributions of marine and terrestrial organic matter to aquatic environments, as the elemental and isotopic compositions of organic matter typically preserve source information (Peters et al., 1978; Monteiro et al., 2012; Meyers, 2014; Sanders et al., 2014).

The combination of results indicates the presence of three distinct layers along the core (Table 1 and Fig. 2), relating to the marine and continental proxies. The bottom layer is characterized by larger contributions of both organic and inorganic marine-sourced material, as evidenced by high Ca/Al, $\delta^{13}C$, and $\delta^{15}N$ values and low C/N. The middle and upper layers present relatively lower and constant values of Ca/Al ratios but differ in terms of organic matter quality proxies. C/N, $\delta^{13}C$, and $\delta^{15}N$ reflect a higher influence of terrestrial/mangrove material in the middle part of the core, and a gradually increasing prevalence of marine organic matter in the upper layers.

The transition from marine to terrestrial sedimentary characteristics between the bottom (1910s to 1920s) and middle (1930s to 1950s) layers of the sediment core is likely the result of man-induced alterations near the coastline, such as extensive river dredging in the early 1910s (Britto et al., 2019) and the construction of the Rio-Petrópolis Road in 1928 (Fig. 2). Human activities can significantly impact the geomorphology, leading to alterations in the source and properties of the river-borne sediment.

The higher clay content in the bottom layers is likely related to the proximity of the site to marine clayey mud flats. The middle layer of the core, which has lower sediment depositional fluxes and clay content, may have been deposited when the material source, e.g., a mud flat that is frequently disturbed by tides and supplies sediments to nearby areas, was further away from the sampling site (Smoak & Patchineelam, 1999). Monteiro et al. (2012) also identified increasing sand contents in the northeastern part of the Guanabara Bay before 1950's, associated with land use changes, such as deforestation, to allow for urban and agriculture growth.

The changing organic matter characteristics between the middle (from 1930's to 1950's) and the most recently deposited layers (from 1960's to 2010's) likely stems from a transition between terrestrial to eutrophic marine sediments. This is evidenced by the C/N, $\delta^{13}C$ and $\delta^{15}N$ values in the upper layer, which are typical for organic matter inputs from algal origin (Peters et al., 1978; Monteiro et al., 2012; Meyers, 2014; Sanders et al., 2014). Eutrophication is further supported by increasing concentrations in P and N along the sediment column.

3.2 Identifying historical stages of Cu contamination

Overall, the data indicates an increasing anthropogenic impact over time. Before 1965, Cu EF and Cu flux were relatively low and stable. In this period, a slight increase (up to 2 $\mu g.cm^{-2}year^{-1}$) coincides with higher terrigenous inputs due to river dredging and the inauguration of the Rio-Petrópolis Road in 1928 (Fig. 2). After 1965, period with eutrophic marine sediments (see Section 3.1), Cu EFs increased up to 3.79 (reached in 1971), corroborating with the significant historical contamination identified by previous studies in the Estrela River sediments (Rebello et al., 1986; Rangel et al., 2011). These results reflect the intense industrialization and population growth in the watershed, paralleled by elevated trace metal contamination and eutrophication in the Guanabara Bay after the 1960's (Alencar, 1980; Godoy et al., 1998; Monteiro et al., 2012).

Based on this context and intervals of Cu EF along the sedimentary core, two stages of Cu contamination were defined to evaluate the evolution of Cu isotopes and speciation (Fig. 2):

- Stage I – landscape changes (22 – 42 cm below SWI – sediment water interface, 1913 – 1965; Cu EF < 2).
- Stage II –intense industrialization and urbanization (0 - 22 cm below SWI, after 1965; Cu EF > 2).

A previous study in Guanabara Bay also identified two analogous phases during the 20^{th} century, one of land use change before the 1950's, succeeded by a phase of significant sewage input (Monteiro et al., 2012).

Cu enrichment is positively correlated to P and $\delta^{15}N$ (Pearson r = 0.78 and 0.59, respectively, $p < 0.05$ for both), suggesting a possible Cu sourcing into the bay by sewage inputs. However, TOC (%) in the sediments did not significantly change between stages, which would be expected during exclusively untreated sewage contamination. Moreover, the stepwise increase in Cu concentrations, in contrast to the more gradual increase in population (Fig.2), suggests the contribution of Cu emissions from punctual industrial sources. Hence, Cu contamination probably results from a mixing between diffuse urban sources and punctual industrial sources (see Section 2.1), which will be further addressed in Section 3.2. This flux is associated with increasing sediment deposition and Al contents

(representative of continental aluminosilicates) during stage II, suggesting land inputs of Cu contaminated particles to the coastal area.

The population growth (Fig. 2), and the observed Cu and P data in stage II may have been influenced by two significant societal factors. The first one is the transition to the creation of the State of Rio in 1975 (de Oliveira & Rodrigues, 2009), which increased the integration, and hence development and industrialization of the region. The second factor is the implementation of the 2nd NDP (National Development Plan) in the early 1970s. It was a strategic economic and development plan created by the Brazilian government to guide the country's growth and progress, which promoted the industrialization and economic development in the State of Rio de Janeiro (de Oliveira & Rodrigues, 2009), leading to higher industrial activities, and hence related pollution.

Subsequently, a gradual decrease of Cu and P fluxes (and buried levels) could be attributed to the implementation of the National Sanitary Plan (PLANASA) in 1971 addressed to improve the caption and treatment of sewage. While there was no reliable information about the sanitation services at the time, it is generally accepted that only about one third of the sewage generated by the population in the hydrographic basin of the Guanabara Bay was treated in 2015, which improved to one half in 2020, according to SNIS (2020).

Second-order fluctuations of Cu observed in the core can be explained as described below. The slight decrease in Cu and P concentrations in the 1980's coincides with the deindustrialization of the Rio de Janeiro State caused by the Brazilian economic woes in this period (de Oliveira & Rodrigues, 2009). Likewise, the later increasing values of Cu concentrations and fluxes from the 1990s reflect the impacts of the regrowth of the Rio de Janeiro industry (de Oliveira & Rodrigues, 2009). Notably, the maximum Cu flux (>12 $\mu g.cm^{-2}.year^{-1}$) reached in 2013 is nearly twice the values reported elsewhere for the Environmental Protection Area located in the opposite side of the Guanabara Bay (Monteiro et al., 2012), which strengthens environmental concerns in this area of the Guanabara Bay (Fries et al., 2019).

3.3 Inferring anthropogenic and natural Cu sources

Both the PCA (Fig. 3) and the plotting of $\delta^{65}Cu$ against 1/Cu (Fig. 4) evidence a binary mixing model between natural and anthropogenic sources. The PCA showed two principal components responding for approximately 70% of the dataset total variance.

The first component (PC1) reflects relative contributions of natural and anthropogenic Cu. The correlations between Cu EF, F1, F2, and P suggests that anthropogenic Cu is present in more mobile and potentially bioavailable forms. The anticorrelation of $\delta^{65}Cu$ with these parameters implies that anthropogenic sources of Cu have a lighter isotope signature than natural sources. Indeed, $\delta^{65}Cu$ values in the present study are lower than most of the $\delta^{65}Cu$ values reported in previous studies for pristine sediments, and in the range of industrial sources of contamination (Fig. 5). Moreover, the sediment samples from the anthropogenic stage II were found to be enriched in ^{63}Cu ($\delta^{65}Cu$= -0.42±0.05‰) compared to the slightly anthropized sediments from stage I ($\delta^{65}Cu$= -0.15±0.18‰; after 1928; Fig. 4).

Similarly, Jeong et al. (2023b) found coastal sediments from Korea impacted by multiple urban and industrial sources with relatively lower Cu isotope values (0.46‰ in Busan compared to 0.73‰ in Shihwa-Incheon). Authors associated this with the influence of industrial and roadway activities, based on $\delta^{65}Cu$ dust from industrial (0.24‰; Jeong et al., 2021a) and urban areas (0.26‰; Jeong and Ra, 2021). Moreover, Jeong et al. (2021a) found road dust with the highest Cu concentrations from industrial areas of Korea with highlighted low $\delta^{65}Cu$ value of -0.12‰ (Jeong and Ra, 2021).

The plotting of $\delta^{65}Cu$ against 1/Cu (Fig. 4) shows a statistically significant correlation (Pearson $r = 0.92$, $p < 0.05$) from the 1930's on, after the inauguration of the Rio-Petrópolis Road. The isotope value of 0.10‰ (1929) is the only within the range of the Upper Continental Crust ($\delta^{65}Cu$ UCC = 0.08±0.17%; Vance et al., 2008; Takano et al., 2014; Thompson et al., 2014; Moynier et al., 2017) and pristine modern sediments around the world (0.29 ±0.37; Little et al., 2017; Araújo et al., 2019a; Ciscato et al., 2019), indicating that this sediment is representative of the major natural source in the mixing model.

The anthropogenic end-member, which probably integrate multiple sources, was estimated to be ~-0.49‰ by linear extrapolation to the origin (i.e., to x =0) of the linear regression between 1/Cu and $\delta^{65}Cu$. This estimation is constrained to a limited number of samples in the model (n = 9), which should be carefully considered. It would be difficult to determine the isotope values of single end-members, since the Estrela River watershed is occupied by multiple punctual sources (see section 2.1), besides diffuse sources from the bay. The presence of industrial sourced material is evident by the ranges of $\delta^{65}Cu$ (Fig. 5) and the stepwise increase in Cu concentrations (Fig. 2). Correlations of Cu EF with P and $\delta^{15}N$ (see Section 3.2), suggest possible Cu sourcing into the bay by sewage

inputs, but to date, there is no record of $\delta^{65}Cu$ from domestic sewage. Araujo et al. (2019) found coastal sediments contaminated by diffuse sources tending to negative $\delta^{65}Cu$ values (down to -0.79‰). Therefore, the value of $\delta^{65}Cu$ ~-0.49‰ reflects the mixing between major punctual industrial sources, and possibly diffuse urban sources.

While the shift in Cu isotope values between the 1930's and 1960's is satisfactorily explained by the mixing of isotopically light contaminated land particles and natural UCC-derived sediment, the bottom layer requires a separate evaluation. The sample from 1913 is enriched in ^{63}Cu (-0.36‰), within the range of $\delta^{65}Cu$ in the anthropogenic period after the 1960's (stage II; Fig 2). Since Cu concentrations in the pre-anthropogenic period (stage I) are mostly natural, it is natural sources or diagenetic processes that have caused this significant isotopic fractionation.

The most straightforward explanation for the isotopic difference between 1913 and 1929 relies on the fact that they are characterized by distinct sediment types, driven by coastline changes (see Section 3.2). The bottom layer (1913) exhibits noticeable differences in $\delta^{13}C$ and Ca/Al (Fig. 4), indicating the presence of distinct natural sources that control $\delta^{65}Cu$, in the absence of significant anthropogenic influence. The second principal component of the PCA, accounting for 28% of the variation in the data, evidences the control between marine and terrestrial influence in the area (Fig. 3).

To summarize, the findings suggest that after the inauguration of the Rio-Petropolis Road, there were increased continental inputs that had specific $\delta^{65}Cu$ background values and high Fe contents (Fig. 2), which are typical for tropical soils (Rieuwerts, 2015). Such inputs, accompanied by coastline changes, overshadowed/drowned the ^{65}Cu depleted marine source. With rapid urbanization and industrialization after the 1960's, this natural continental source was mixed with Fe depleted land material, contaminated by isotopically light Cu and further transported to the coastal zone (Fig. 2).

3.4 Geochemical partition of anthropogenic Cu: a speciation analysis on Cu mobility and bioavailability

The most significant change in the geochemical distribution of Cu was observed between Stages I and II, which is dominated by labile forms of anthropogenic Cu (average $F4_{Stage\ I}$ = 81.70%; average $F4_{Stage\ II}$= 65.08%). Leal & Rebello (1993) found a similar enrichment of bioavailable Cu in recent sediments from the Estrela River. In other words, anthropogenic Cu from the continent is reallocated within reactive phases in mangroves.

A set of various processes such as mineral dissolution, mineral precipitation, compaction, organic matter degradation, and bacterial activity, involved in diagenesis can alter internal Cu distribution among geochemical sediment phases. However, this is unlikely, since particulate matter from the Estrela River, once deposited in the sediments, undergoes only limited transformation (Leal and Rebello, 1993). Indeed, Cu diffusion from sediments to water column through upwelling pore waters in anoxic coastal sediments tend to be low and not substantial to alter the bulk sediments phases. For instance, Rangel et al. (2011) detected nearly depletion of soluble Cu in sediments from the Estrela River. This suggests that diagenetic processes do not drive significant isotopic fractionation in the area, since it requires substantial loss of Cu from the bulk sediments to water or biota. Moreover, previous works show that Cu isotope variability in particulate material tend to be conservative across fluvial estuarine biogeochemical processes, being well described in terms of source mixing models (Petit et al., 2008; Guinoiseau et al. 2018; Araújo et al., 2019a). Finally, the profile of ^{210}Pb in dated sediment layers is consistent with the historical changes in Cu concentrations during the period of industrialization and urbanization of a bay (Alencar, 1980; Monteiro et al., 2012), suggesting the preservation of geochemical records in the mud flats. Anyway, estimates of potential isotope fractionation caused by sorption process do not unsustain a diagenetic effect on bulk sediments from both stages (details the Supplementary Material: Geochemical processes assessed by partitioning of Cu).

Finally, It is worth noting that the lowest relative contents of non-mobile Cu (F4 of 60%) were observed in 1981, which was accompanied by the lowest δ^{65}Cu of the core (-0.51‰), and relatively low Cu flux (5.6 $\mu g.cm^{-2}.year^{-1}$; Fig 2). We suggest that inputs of isotopically light and more bioavailable anthropogenic Cu, combined with the loss of UCC-derived ^{65}Cu-rich sediments due to deforestation, could be responsible for this observation.

4. Conclusions

This study demonstrated that Cu isotopes combined with established proxies for organic and inorganic matter in mangrove sediments allow to identify landscape changes. The variation in Cu isotopes observed in the mangrove sediment profile can be explained by the relative contribution of natural and anthropogenic sources. The natural Cu include marine and terrestrial end-members with distinct isotope compositions resulting from

underlying biogeochemical processes. The origin of the terrigenous Cu isotope composition is likely attributed to weathering, while the processes that give rise to the marine Cu isotope composition remain unclear.

Cu isotopes were found to be valuable tools for tracking anthropogenic inputs into mangrove sediments. This study found that land-derived particles affected by multiple anthropogenic sources in coastal areas present distinguishable Cu isotope compositions. This is a pertinent application to regulate emission policies, particularly in areas under the multiple environmental pressures, such as Guanabara Bay. Solid partition data indicates that anthropogenic inputs increase the proportion of Cu in its labile forms, resulting in higher mobility and bioavailability.

In many coastal areas, such as Guanabara Bay, it is challenging to assess each anthropogenic source. Here we show the possibility of differentiating anthropogenic pools, as opposed to natural sources, in complex urban scenarios where the datasets pose logistical and resource limitations. This is also relevant for cases in which sediments were historically contaminated by closed or controlled facilities, preventing the isotope analysis of specific sources. In summary, trace metal stable isotopes can be useful tools for tracing sources when multiple primary sources - both contemporary and legacy - combine into a resultant mixture with distinct isotope signatures. Further studies with complementary compartments, such as porewaters, can help elucidate mechanisms of inter-compartmental transfers and Cu incorporation into by local benthonic fauna. Studying mangrove systems under distinct environmental conditions and degrees of anthropogenic pressure can also provide a more comprehensive view in the role of these ecosystems in Cu cycling. Finally, to enhance the understanding of source apportionment in future studies within this study area, it is recommended to investigate runoff patterns and perform end-member characterization.

5. Competing interests

The contact author has declared that neither him nor co-authors have any competing interests or personal relationships that could influence the work reported in this paper.

6. Acknowledgements

We thank the anonymous reviewers for valuable suggestions that substantially improved the final version of this study. This study was supported in part by the Coordenação de Aperfeiçoamento Pessoal de Nível Superior (CAPES), Brazil (Finance

Code 001). J. B. acknowledges the financial support from CAPES (grant number 88887.483826/2020-00). W.M. acknowledges the financial support from National Research Council (CNPq-Brazil) and PRINT-UFF-FEEDBACKS grant CAPES (grant number 88887.310301/2018-00).

7. References

AGEVAP, 2021. Atlas da Região Hidrográfica V (electronic book): Baía de Guanabara e sistemas lagunares de Maricá e Jacarépaguá / organização João Paulo Paulino Coimbra. 1 ed, Resende. Available at < https://comitebaiadeguanabara.org.br/wp-content/uploads/2022/09/Atlas_CBH-BG.pdf>. Accessed in February 2023.

Albarède, F., 2004, The stable isotope geochemistry of copper and zinc: Reviews in Mineralogy and Geochemistry, v. 55, no. 1, p. 409–427, doi:10.2138/gsrmg.55.1.409.
Alongi, D. M., 2017. Micronutrients and mangroves: Experimental evidence for copper limitation. Limnol. Oceanogr., 62(6), 2759–2772.

Alencar, E., 1980. Guanabara Bay: neglect and resistance. 1st ed. translation by Nadge Medeiros de Souza – Rio de Janeiro: Fundação Heinrich Böll / Mórula, 2016.

AN, 2016. Nacional Archive. Memory of the Brazilian Public Administration. Gunpowder Factory. Available at http://mapa.an.gov.br/index.php/menu-de-categorias-2/319-fabrica-de-polvora-1822-1889. Accessed in May 2021.

Appleby, P. G., and F. Oldfield, 1978, The calculation of lead-210 dates assuming a constant rate of supply of unsupported 210PB to the sediment: CATENA, 5(1), 1–8, doi:10.1016/s0341-8162(78)80002-2.

Araújo, D. F., Boaventura, G. R., Machado, W., Viers, J., Weiss, D., Patchineelam, S. R., Ruiz, I., Rodrigues, A. P.., Babinski, M. Dantes, E., 2017. Tracing of anthropogenic zinc sources in coastal environments using stable isotope composition: Chem. Geol., 449, 226–235, doi:10.1016/j.chemgeo.2016.12.004.

Araújo, D. F., W. Machado, D. Weiss, D. S. Mulholland, J. Garnier, C. E. Souto-Oliveira, and M. Babinski, 2018. Zinc isotopes as tracers of anthropogenic sources and

biogeochemical processes in contaminated mangroves: Appl. Geochem., 95, 25–32, doi:10.1016/j.apgeochem.2018.05.008.

Araújo, D. F.; Ponzevera, E., Briant, N.; Knoery, J.; Sireau, T.; Mojtahid, M.; Metzger, E.; Brach-Papa, C., 2019a. Assessment of the metal contamination evolution in the Loire estuary using Cu and Zn stable isotopes and geochemical data in sediments. Mar. Pollut. Bull., 143, 12-23, doi:10.1016/j.marpolbul.2019.04.034.

Araújo, D. F.; Ponzevera, E.; Briant, J.; Bruzac, S.; Sireau, T.; Brach-Papa, C., 2019b. Copper, zinc and lead isotope signatures of sediments from a mediterranean coastal bay impacted by naval activities and urban sources. Appl. Geochem., 111, 104440, doi:10.1016/j.apgeochem.2019.104440.

Babcsányi, I., Imfeld, G., Granet, M., & Chabaux, F., 2014. Copper stable isotopes to trace copper behavior in wetland systems. Environ. Sci. Technol., 48(10), 5520–5529, doi:10.1021/es405688v.

Babcsányi, I., Chabaux, F., Granet, M., Meite, F., Payraudeau, S., Duplay, J., Imfeld, G., 2016. Copper in soil fractions and runoff in a vineyard catchment: Insights from copper stable isotopes. Sci. Total Environ., 557-558, 154-162, doi:10.1016/j.scitotenv.2016.03.037.

Balistrieri, L., Borrok, D., Wanty, R., Ridley, W., 2008. Fractionation of Cu and Zn isotopes during adsorption onto amorphous Fe (III) oxyhydroxide: Experimental mixing of acid rock drainage and ambient river water. Geochim. Cosmochim. Acta., 72(2), 311-328, doi:10.1016/j.gca.2007.11.013.

Baptista-Neto, J. A., Smith, B. J., Mcallister, J. J., 2000. Sedimentological evidence of human impact on a nearshore environment: Jurujuba Sound, Rio de Janeiro State, Brazil. Applied Geography, 19, 2, 153–177, doi:10.1016/S0143-6228(98)00041-1.

Bastakoti, U., Robertson, J., Marchand, C., & Alfaro, A. C., 2019, October. Mangrove removal: Effects on trace metal concentrations in temperate estuarine sediments. Mar. Chem., 216, 10368, doi:10.1016/j.marchem.2019.103688.

Bigalke, M. Weyer, S. Kobza, J. Wilcke, W., 2010. Stable Cu and Zn isotope ratios as tracers of sources and transport of Cu and Zn in contaminated soil. Geochim. Cosmochim. Acta., 74, 6801 – 6813, doi:10.1016/j.gca.2010.08.044.

603 Blotevogel, S., Oliva, P., Sobanska, S., Viers, J., Vezin, H., Audry, S., Prunier, J.,
604 Darrozes, J., Orgogozo, L., Courjault-Radé, P., Schreck, E., 2018. The fate of Cu
605 pesticides in vineyard soils: A case study using δ65Cu isotope ratios and EPR analysis.
606 Chem. Geol., 477, 35–46, doi:10.1016/j.chemgeo.2017.11.032.

607 Borges, A de C., 2006. Dinâmica do fósforo em sedimentos de manguezal em um
608 gradiente de degradação da vegetação. MS Dissertation, Universidade Federal
609 Fluminense.

610 Borges, A. C., Sanders, C. J., Santos, H. L., Araripe, D. R., Machado, W.,
611 Patchineelam, S. R., 2009. Eutrophication history of Guanabara Bay (SE Brazil) recorded
612 by phosphorus flux to sediments from a degraded mangrove area. Mar. Pollut. Bull., 58,
613 11, 1750-1754, doi:10.1016/j.marpolbul.2009.07.025.

614 Briant, N., Freydier, R., Elbaz-Poulichet, F., Chouvelon, T., Knoery, J., 2016. Les
615 isotopes stables du Cu: traceurs des sources de pollution ou des processus géochimiques?
616 Perspectives pour le mercure. 28ème Forum des Jeunes Océanographes - du 18 au 20 mai,
617 Cherbourg.

618 Briant, N., Freydier, R., Araújo, D. F., Delpoux, S., Elbaz-Poulichet, F., 2022, Cu
619 isotope records of Cu-based antifouling paints in sediment core profiles from the largest
620 European Marina, the Port Camargue: Sci. Total Environ., 849, 157885,
621 doi:10.1016/j.scitotenv.2022.157885.

622 Britto, A. L., Quintslr, S., Pereira, M. da. S., 2019. Baixada Fluminense: Fluvial
623 and Social Dynamics in the Constitution of a Territory. Rev. Bras. Hist, 39(81),
624 10.1590/1806-93472019v39n81-03.

625 Campos, B. G.; Cruz, A. C. F.; Buruaem, L. M.; Rodrigues, A. P. C.; Machado, W.
626 T. V.; Abessa, D. M. S., 2016. Using a tiered approach based on ecotoxicological
627 techniques to assess the ecological risks of contamination in a subtropical estuarine
628 protected area. Sci. Total Environ., 544, 564-573, doi: 10.1016/j.scitotenv.2015.11.124.

629 Ciscato, E. R., Bontognali, T. R. R., Poulton, S. W., Vance, D., 2019. Copper and
630 its Isotopes in Organic-Rich Sediments: From the Modern Peru Margin to Archean
631 Shales. Geosciences, 9, 325, doi:10.3390/geosciences9080325.

632 Clark, M. W., Mcconchie, D., Lewis, D. W.; Saenger, P., 1998. Redox stratification
633 and heavy metal partitioning in Avicennia-dominated mangrove sediments: a
634 geochemical model. Chem. Geol., 149, 147-171, doi:10.1016/S0009-2541(98)00034-5.

635 Clayton, R. E., Hudson-Edwards, K. A., Houghton, S. L., 2005. Isotopic effects
636 during Cu sorption onto goethite. Goldschmidt Conference Abstracts 2005 - Non-
637 Traditional Stable Isotopes.

638 De Oliveira, A., Rodrigues, A. O., 2009. Industrialização na periferia da região
639 metropolitana do Rio de Janeiro: novos paradigmas para velhos problemas. Semest.
640 Econ., 12(24), 127-143,

641 Defew, L. H., Mair, J. M., & Guzman, H. M., 2005. An assessment of metal
642 contamination in mangrove sediments and leaves from Punta Mala Bay, Pacific Panama.
643 Mar. Pollut. Bull., 50(5), 547–552, doi:10.1016/j.marpolbul.2004.11.047.

644 Dong, S., Ochoa Gonzalez, R., Harrison, R. M., Green, D., North, R., Fowler, G.,
645 & Weiss, D., 2017. Isotopic signatures suggest important contributions from recycled
646 gasoline, road dust and non-exhaust traffic sources for copper, zinc and lead in PM 10 in
647 London, United Kingdom. Atmos. Environ., 165, 88–98,
648 doi:10.1016/j.atmosenv.2017.06.020.

649 Dótor-Almazán, A., Armienta-Hernández, M. A., Talavera-Mendoza, O., & Ruiz,
650 J., 2017. Geochemical behavior of Cu and sulfur isotopes in the tropical mining region of
651 Taxco, Guerrero (southern Mexico). Chem. Geol., 471, 1–12,
652 doi:10.1016/j.chemgeo.2017.09.005.

653 El Azzi, D., Viers, J., Guiresse, M., Probst, A., Aubert, D., Caparros, J., Charles,
654 F., Guizien, K., Probst, J. L., 2013. Origin and fate of copper in a small Mediterranean
655 vineyard catchment: new insights from combined chemical extraction and δ65Cu isotopic
656 composition. Sci. Total Environ, 463-464, 91–101, doi:10.1016/j.scitotenv.2013.05.058.

657 Esri, 2018. "Land Cover" [basemap]. Scale Not Given. "Global Land Cover Map".
658 Available at <https://livingatlas.arcgis.com/landcoverexplorer/> Acessed in March 2023.

659 Fries, A. S., Coimbra, J. P., Nemazie, D. A., Summers, R. M., Azevedo, J. P. S.,
660 Filoso, S., Newton, M., Gelli, G., de Oliveira, R. C. N., Pessoa, M. A. R., Dennison, W.
661 C., 2019. Guanabara Bay ecosystem health report card: Science, management, and

governance implications. Reg. Stud. Mar. Sci., 25, 100474, doi:10.1016/j.rsma.2018.100474.

Godoy, J. M., Moreira, I., Braganca, M. J., Wanderley, C., Mendes, L. B., 1998. A study of Guanabara Bay sedimentation rates. J. Radioanal. Nucl. Chem., 227(1), 157–160, doi:10.1007/BF02386450.

Guinoiseau, D., Bouchez, J., Gélabert, A., Louvat, P., Moreira-Turcq, P., Filizola, N., & Benedetti, M. F., 2018. Fate of particulate copper and zinc isotopes at the Solimões-Negro river confluence, Amazon Basin, Brazil. Chem. Geol., 489, 2017, 1–15. https://doi.org/10.1016/j.chemgeo.2018.05.004.

Harbison, P., 1986. Mangrove Muds—A Sink and a Source for Trace Metals. Mar. Pollut. Bull., 17, 246-250, doi:10.1016/0025-326X(86)90057-3.

He, X., Chen, G., Fang, Z., Liang, W., Li, B., Tang, J., Sun, Y., & Qin, L., 2020. Source identification of chromium in the sediments of the Xiaoqing River and Laizhou Bay: A chromium stable isotope perspective. Environ. Pollut., 264, 114686, doi:10.1016/j.envpol.2020.114686.

Huang, S., Jiang R., Song, Q., Zhang, Y., Huang, Q., Su, B., Chen, Y., Huo, Y., Lin, J., 2020. Study of mercury transport and transformation in mangrove forests using stable mercury isotopes. Sci. Total Environ., 704, 135928, doi:10.1016/j.scitotenv.2019.135928.

Huang, S., Jiang R., Song, Q., Zhao, Y., Lv, S., Zhang, Y., Huo, Y., Chen, Y., 2021. The Hg behaviors in mangrove ecosystems revealed by Hg stable isotopes: A case study of maowei mangrove. Environ. Sci. Pollut. Res., 29(17), 25349–25359, doi:10.1007/s11356-021-17744-4.

Huerta-Diaz, M. A., Morse, J. W., 1992. Pyritization of trace metals in anoxic marine sediments. Geochim. Cosmochim. Acta, 56, 2681–2702, doi:10.1016/0016 7037(92)90353-K.

IBGE (2021a). Panorama Duque de Caxias. Available at <https://cidades.ibge.gov.br/brasil/rj/duque-de-caxias/panorama>. Accessed onNovember 2022.

IBGE (2021b). Panorama Magé. Available at <https://cidades.ibge.gov.br/brasil/rj/mage/panorama>. Accessed onNovember 2022.

Jeong, H., Choi, J. Y., & Ra, K. (2021a). Heavy metal pollution assessment in stream sediments from urban and different types of industrial areas in South Korea. Soil and Sediment Contamination: An International Journal, 30(7), 804-818.

Jeong, H., & Ra, K. (2021). Characteristics of potentially toxic elements, risk assessments, and isotopic compositions (Cu-Zn-Pb) in the PM10 fraction of road dust in Busan, South Korea. Atmosphere, 12(9), 1229.

Jeong, H., Araújo, D. F., Garnier, J., Mulholland, D., Machado, W., Cunha, B., Ponzevera, E., 2023a. Copper and lead isotope records from an electroplating activity in sediments and biota from Sepetiba Bay (southeastern Brazil). Mar. Pollut. Bull., 190, 114848, doi: 10.1016/j.marpolbul.2023.114848.

Jeong, H., Lee, Y., Moon, H. B., & Ra, K. (2023b). Characteristics of metal pollution and multi-isotopic signatures for C, Cu, Zn, and Pb in coastal sediments from special management areas in Korea. Marine Pollution Bulletin, 188, 114642.

Kjerfve, B., Ribeiro, C.H.A., Dias, G.T.M., Filippo, A.M., Da Silva Quaresma, V., 1997. Oceanographic characteristics of an impacted coastal bay: Baía de Guanabara, Rio de Janeiro, Brazil. Continental Shelf Research 17, 1609–1643., doi:10.1016/S0278-4343(97)00028-9.

Komárek, M., Ettler, V., Chratsný, V., Mihaljevič, M., 2008. Lead isotopes in Environmental Sciences: A Review. Environ. Int., 34(4), 562–577, doi:10.1016/j.envint.2007.10.005.

Lacerda, L. D. de, Ward, R. D., Borges, R., Ferreira, A. C., 2022. Mangrove trace metal biogeochemistry response to global climate change. Front. for. glob. change, 5, 817992, doi:10.3389/ffgc.2022.817992.

Leal, M. L. S., Rebello, A. de L., 1993. Remobilisation of anthropogenic copper deposited in sediments of a tropical estuary. Chem. Speciation Bioavailability, 5(1), 31-39, doi: 10.1080/09542299.1993.11083200.

Lessa, Carlos, 2000. O Rio de todos os Brasis: Uma reflexão em busca de auto-estima. Rio de Janeiro: Record, 478p.

721 Li, W., Jackson, S., Pearson, N. J., Alard O., Chappell B. W., 2009. The Cu isotopic
722 signature of granites from the Lachlan Fold Belt, SE Australia. Chem. Geol., 258, 38–49,
723 doi: 10.1016/j.chemgeo.2008.06.047.

724 Little, S. H., Vance, D., Walker-Brown, C., & Landing, W. M. (2014). The oceanic
725 mass balance of copper and zinc isotopes, investigated by analysis of their inputs, and
726 outputs to ferromanganese oxide sediments. Geochimica et Cosmochimica Acta, 125,
727 673-693.

728 Little, S. H., Vance, D., McManus, J., Severmann, S., & Lyons, T. W., 2017.
729 Copper isotope signatures in modern marine sediments. Geochim. Cosmochim. Acta.,
730 212, 253–273, doi:10.1016/j.gca.2017.06.019.

731 Little, S. H., Archer, C., Milne A., Schlosser, C., Achterberg, E. P., Lohan M. C.,
732 Vance, D., 2018. Paired dissolved and particulate Stage Cu isotope distributions in the
733 South Atlantic. Chem. Geol., 502, 29–43, doi:10.1016/j.chemgeo.2018.07.022.

734 Loring, D. H. (1991). Normalization of heavy-metal data from estuarine and coastal
735 sediments. ICES Journal of Marine Science, 48(1), 101-115.

736 Machado, W., Moscatelli, M., Rezende, L. G., Lacerda, L. D., 2002a. Mercury,
737 zinc, and copper accumulation in mangrove sediments surrounding a large landfill in
738 southeast Brazil. Environ. Pollut., 120, 455–461, doi: 10.1016/s0269-7491(02)00108-2

739 Machado, W., Silva-Filho, E. V., Oliveira, R. R., L. G., Lacerda, L. D., 2002b.
740 Trace metal retention in mangrove ecosystems in Guanabara Bay, SE Brazil. Mar. Pollut.
741 Bull., 44(11), 1277–1280, doi: 10.1016/S0025-326X(02)00232-1.

742 Machado, W., Santelli, R.E., Carvalho, M.F., Molisani, M.M., Barreto, R.C.,
743 Lacerda, L.D., 2008. Relation of reactive sulfides with organic carbon, iron, and
744 manganese in anaerobic mangrove sediments: implications for sediment suitability to trap
745 trace metals. J. Coast. Res. 4, 25–32., doi:10.2112/06-0736.1.

746 Machado, W., Rodrigues, A.P.C., Bidone, E.D., Sella, S.M., Santelli, R.E., 2011.
747 Evaluation of Cu potential bioavailability changes upon coastal sediment resuspension:
748 an example on how to improve the assessment of sediment dredging environmental risks
749 Environ. Sci. Pollut. Res., 18, 1033-1036. https:// doi:101007/s11356-011-0517-1.

Machado, W., Borrelli, N. L., Ferreira, T. O., Marques, A. G. B., Osterrieth, M., Guizan, C., 2014. Trace metal pyritization variability in response to mangrove soil aerobic and anaerobic oxidation processes. Mar. Pollut. Bull., 79, doi: 365-370, 10.1016/j.marpolbul.2013.11.016.

Marchand, C., Lallier-Vergès, E., Baltzer, F., Albéric, P., Daniel, C., Baillif, P., 2006. Heavy metals distribution in mangrove sediments along the mobile coastline of French Guiana. Mar. Chem., 98(1), 1-17, doi:10.1016/j.marchem.2005.06.001.

Mathur, R., Jin, L., Prush, V., Paul, J., Ebersole, C., Fornadel, A., Brantley, S., 2012. Cu isotopes and concentrations during weathering of black shale of the Marcellus Formation, Huntingdon County, Pennsylvania (USA). Chem. Geol., 304-305, 175–184, doi:10.1016/j.chemgeo.2012.02.015.

Meyers, P. A. (1994). Preservation of elemental and isotopic source identification of sedimentary organic matter. Chem. Geol., 114, 3-4, 289-302, doi: 10.1016/0009-2541(94)90059-0.

Monteiro, F. F., Cordeiro, R. C., Santelli, R. E., Machado, W. T. V., Evangelista, H., Villar, L. S., Viana, L. C. A., Bidone, E. D., 2012. Sedimentary geochemical record of historical anthropogenic activities affecting Guanabara Bay (Brazil) environmental quality. Environ. Earth Sci., 65(6), 1661–1669, doi: 10.1007/s12665-011-1143-4.

Moynier, F., Vance, D., Fujii, T., Savage, P., 2017. The isotope geochemistry of zinc and copper. Rev. Mineral. Geochem. 2017, 82, 543–600, doi: 10.2138/rmg.2017.82.13.

Novak, M., Sipkova, A., Chrastny, V., Stepanova, M., Voldrichova, P., Veselovsky, F., Prechova, E., Blaha, V., Curik, J., Farkas, J., Erbanova, L., Bohdalkova, L., Pasava, J., Mikova, J., Komarek, A., & Krachler, M., 2016. Cu-Zn isotope constraints on the provenance of air pollution in Central Europe: Using soluble and insoluble particles in snow and rime. Environ. Pollut., 218, 1135–1146, doi:10.1016/j.envpol.2016.08.067.

Peters, K. E., Sweeney, R. E. and Kaplan, I. R., 1978. Correlation of carbon and nitrogen stable isotope ratios in sedimentary organic matter. Limnology and Oceanography 23, 598-604, doi: 10.4319/lo.1978.23.4.0598.

Petit, J. C. J., de Jong, J., Chou, L., Mattielli, N., 2008. Development of Cu and Zn isotope MC-ICP-MS measurements: application to suspended particulate matter and

781 sediments from the Scheldt estuary. Geostand. Geoanal. Res., 32(2), 149–166, doi:
782 10.1111/j.1751-908X.2008.00867.x.

783 Petit, J. C. J., Schäfer, J., Coynel, A., Blanc, G., Deycard, V. N., Derriennic, H.,
784 Lanceleur, L., Dutruch, L., Bossy, C., Mattielli, N., 2013. Anthropogenic sources and
785 biogeochemical reactivity of particulate and dissolved Cu isotopes in the turbidity
786 gradient of the Garonne. Chem. Geol., 359, 125135, doi:10.1016/j.chemgeo.2013.09.019.

787 Pokrovsky, O. S., Viers, J., Emnova, E. E., Kompantseva, E. I., Freydier, R., 2008.
788 Copper isotope fractionation during its interaction with soil and aquatic microorganisms
789 and metal oxy(hydr)oxides: Possible structural control. Geochim. Cosmochim. Acta.,
790 2(7), 1742-1757, doi:10.1016/j.gca.2008.01.018.

791 Queiroz, H., M., Barbosa, I. O., Bragantini, F., Fandiño, V. A., Bernardino, A. F.,
792 Barcellos, D., Ferreira, A. D., Gomes, L. E. de O., Ferreira, T. O., 2022. Degraded
793 mangroves as sources of trace elements to aquatic environments. Mar. Pollut. Bull., 181,
794 113834, doi: 10.1016/j.marpolbul.2022.113834.

795 Rangel, C. M. A., Neto, J. A. B., Fonseca, E. M., Macalister, J., Smith, B. J., 2011.
796 Study of heavy metal concentration and partitioning in the Estrela River: implications for
797 the pollution in Guanabara Bay - SE Brazil. An. Acad. Bras., 83(3), 801-815,
798 doi:10.1590/S0001-37652011005000020.

799 Rauret, G., López-Sánchez, J. F., Sahuquillo, A., Rubio, R., Davidson, C., Ure, A.,
800 & Quevauviller, P., 1999. Improvement of the BCR three step sequential extraction
801 procedure prior to the certification of new sediment and soil reference materials. J.
802 Environ. Monit., 1(1), 57-61, doi:10.1039/A807854H.

803 Rebello, A. de L., Haekel, W., Moreira, I., Santelli, R., Schroeder, F., 1986. The
804 fate of heavy metals in an estuarine tropical system. Mar. Chem., 18(2-4), 215-225, doi:
805 10.1016/0304-4203(86)90009-5.

806 Rieuwerts, J. S., 2015. The mobility and bioavailability of trace metals in tropical
807 soils: a review. Chemical Speciation & Bioavailability, 19(2), 75-85, doi:
808 10.3184/095422907X211918.

809 Roebbert, Y., Rabe, K., Lazarov, M., Schuth, S., Schippers, A., Dold, B., & Weyer,
810 S., 2018. Fractionation of Fe and Cu isotopes in acid mine tailings: Modification and
811 application of a sequential extraction method. Chem. Geol., 493(May), 67–79.

812 doi:10.1016/j.chemgeo.2018.05.026.

813 Rudnick, R. L., Gao, S., Holland, H. D., & Turekian, K. K., 2003. Composition of
814 the continental crust. Treatise Geochem., 3, 1-64, doi:10.1016/B0-08-043751-6/03016-4.

815 Ryan, B. M., Kirby, J. K., Degryse, F., Scheiderich, K., & McLaughlin, M. J.
816 (2014). Copper isotope fractionation during equilibration with natural and synthetic
817 ligands. Environmental science & technology, 48(15), 8620-8626.

818 Sanders, C. J., Eyre, B. D., Santos, I. R., Machado, W., Luiz-Silva, W., Smoak, J.
819 M., Breithaupt, J. L., Ketterer, M. E., Sanders, L., Marotta, H., Silva-Filho, E., 2014.
820 Elevated rates of organic carbon, nitrogen, and phosphorus accumulation in a highly
821 impacted mangrove wetland. Geophys. Res. Lett., 41(7), 2475-2480,
822 doi:10.1002/2014GL059789.

823 Smoak, J. M., & Patchineelam, S. R., 1999. Sediment mixing and accumulation in
824 a mangrove ecosystem: evidence from ^{210}Pb, ^{234}Th and ^{7}Be. Mangroves Salt Marshes,
825 3(1), 17-27, doi:10.1023/A:1009979631884.

826 Song, S., Mathur, R., Ruiz, J., Chen, D., Allin, N., Guo, K., & Kang, W. (2016).
827 Fingerprinting two metal contaminants in streams with Cu isotopes near the Dexing Mine,
828 China. Science of the Total Environment, 544, 677-685.

829 SNIS, 2020. National Sanitation Information System. Annual diagnosis of water
830 and sewage (reference year 2020). Available at http://antigo.snis.gov.br/diagnostico-
831 anual-agua-e-esgotos. Accessed on September 2021.

832 Soares-Gomes, A., da Gama, B.A.P., Baptista Neto, J.A., Freire, D.G., Cordeiro,
833 R.C., Machado, W., Bernardes, M.C., Coutinho, R., Thompson, F.L., Pereira, R.C., 2016.
834 An environmental overview of Guanabara Bay, Rio de Janeiro. Regional Studies in
835 Marine Science 8, 319–330. https://doi.org/10.1016/j.rsma.2016.01.009.

836 Souto-Oliveira, C. E., Babinski, M., Araújo, D. F., & Andrade, M. F., 2018. Multi-
837 isotopic fingerprints (Pb, Zn, Cu) applied for urban aerosol source apportionment and
838 discrimination. Sci. Total Environ., 626, 1350–1366,
839 doi:10.1016/j.scitotenv.2018.01.192.

840 Souto-Oliveira, C. E., Babinski, M., Araújo, D. F., Weiss, D. J., Ruiz, I. R., 2019.
841 Multiisotope approach of Pb, Cu and Zn in urban aerosols and anthropogenic sources

improves tracing of the atmospheric pollutant sources in megacities. Atmos. Environ. 198, 427–437, doi: 10.1016/j.atmosenv.2018.11.007.

Sullivan, K., Layton-Matthews, D., Leybourne, M., Kidder, J., Mester, Z., & Yang, L. (2020). Copper isotopic analysis in geological and biological reference materials by MC-ICP-MS. Geostandards and Geoanalytical Research, 44(2), 349-362.

Takano, S., Tanimizu, M., Hirata, T., Sohrin, Y., 2014. Isotopic constraints on biogeochemical cycling of copper in the ocean. Nat. Commun, 5, 5663, doi:10.1038/ncomms6663 (2014).

Tang, D., Luo, S., Deng, S., Huang, R., Chen, B., & Deng, Z., 2022. Heavy metal pollution status and deposition history of mangrove sediments in Zhanjiang Bay, China. Front. Mar. Sci., 9,989584, doi:10.3389/fmars.2022.989584.

Thapalia, A., Borrok, D. M.; Van Metre, P. C., Musgrove, M., Landa, E. R., 2010. Zn and Cu isotopes as tracers of anthropogenic contamination in a sediment core from an urban lake. Environ. Sci. Technol., 44(5), 1544-50, doi: 10.1021/es902933y.

Thompson, C. M., Ellwood, M. J., 2014. Dissolved copper isotope biogeochemistry in the Tasman Sea, SW Pacific Ocean. Mar. Chem, 165, 1–9, doi: 10.1016/j.marchem.2014.06.009.

Tessier, A., Campbell, P.G.C., Bisson., M. (1979). Sequential extraction procedure for the speciation of particulated metals. Anal. Chem., 51, 844-851, doi: doi.org/10.1021/ac50043a017

Tonhá, M. S. Ferreira, Garnier, J., A. D., Cunha, B. C. A., Machado, Dantas E. L., Araújo, R., Kutter, V. T., Bonnet, M., Seyler, P., 2020 Behavior of metallurgical zinc contamination in coastal environments: A survey of Zn from electroplating wastes and partitioning in sediment. Sci. Total Environ., 743, 140610, doi: 10.1016/j.scitotenv.2020.140610.

Tonhá, M. S., Araújo, D. F., Araújo, R., Cunha, B. C. A., Machado, W., Portela, J. F., Souza, J. P. R., Carvalho, H. K., Dantas, E. L., Roig, H. L., Seyler, P., Garnier, J., 2021. Trace Metal Dynamics in an industrialized Brazilian River: A combined application of Zn isotopes, geochemical partitioning, and multivariate statistics. J. Environ. Sci., 101, 313-325, doi: 10.1016/j.jes.2020.08.027.

872 Vance, D., Archer, C., Bermin, J., Perkins, J., Statham, P. J., Lohan, M. C.,
873 Ellwood, M. J., Mills, R. A., 2008. The copper isotope geochemistry of rivers and the
874 oceans. Earth Planet. Sci. Lett., 274, 204–213, doi: 10.1016/j.epsl.2008.07.026.

875 Vance, D., Matthews, A., Keech, A., Archer, C., Hudson, G., Pett-Ridge, J., &
876 Chadwick, O. A., 2016. The behaviour of Cu and Zn isotopes during soil development:
877 Controls on the dissolved load of rivers. Chem. Geol., 445, 36–53, doi:
878 10.1016/j.chemgeo.2016.06.002.

879 Viers, J., Grande Gil, J. A., Zouiten, C., Freydier, R., Masbou, J., Valente, T., Torre,
880 M. L. de la, Destrigneville, C., & Pokrovsky, O. S., 2018. Are Cu isotopes a useful tool
881 to trace metal sources and processes in acid mine drainage (AMD) context?
882 Chemosphere, 193, 1071–1079, doi:10.1016/j.chemosphere.2017.11.133.

883 Wang, L., Jin, Y., Weiss, D. J., Schleicher, N. J., Wilcke, W., Wu, L., Guo, Q.,
884 Chen, J., O'Connor, D., Hou, D., 2021. Possible application of stable isotope
885 compositions for the identification of metal sources in soil. Journal of Hazardous
886 Materials, 407, 125812, doi:10.1016/j.jhazmat.2020.124812.

887 Weiss, D. J., Rehkämper, M., Schoenberg, R., Mclaughlin, M., Kirby, J., Campbell,
888 P. G. C., Arnold, T., Chapman, J., Peel, K.; Gioia, S., 2008. Application of nontraditional
889 stable-isotope systems to the study of sources and fate of metals in the environment.
890 Environ. Sci. Technol., 42(3), 655-64, doi: 10.1021/es0870855.

891 Wiederhold, J. G., 2015. Metal stable isotope signatures as tracers in environmental
892 geochemistry. Environ. Sci. Technol., 49(5), 2606–2624, doi:10.1021/es504683e.

893 Xia, B., Huang, Y., Pei, X., Liu, C., & Protection, G., 2022. Application of Cu
894 isotopes to identify Cu sources in soils impacted by multiple anthropogenic activities
895 Application of Cu isotopes to identify Cu sources in soils. doi:10.2139/ssrn.4153317.

896 Zhong, Q., Zhou, Y., Tsang., D. C. W., Liu, J., Yang. X., Yin, M., Wu, S., Wang,
897 J., Xiao, T., Zhang., Z., 2020. Cadmium isotopes as tracers in environmental studies: A
898 Review. Sci. Total Environ., 736, 139585, doi:10.1016/j.scitotenv.2020.139585.

899 Zhu, X.K. et al., 2002. Mass fractionation processes of transition metal isotopes.
900 Earth Planet. Sci. Lett., 200: 47-62, doi:10.1016/S0012-821X(02)00615-5.

901

902

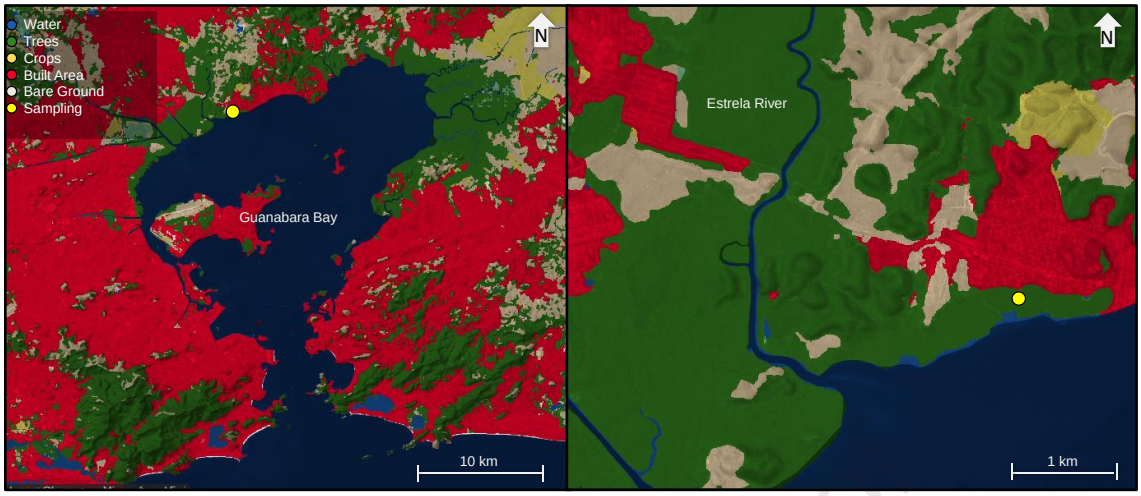

903
904 Figure 1 - Location of the sampling point and land occupation of its surroundings in Guanabara Bay (SE
905 Brazil). Basemap source: Esri (2018)

906

907

908

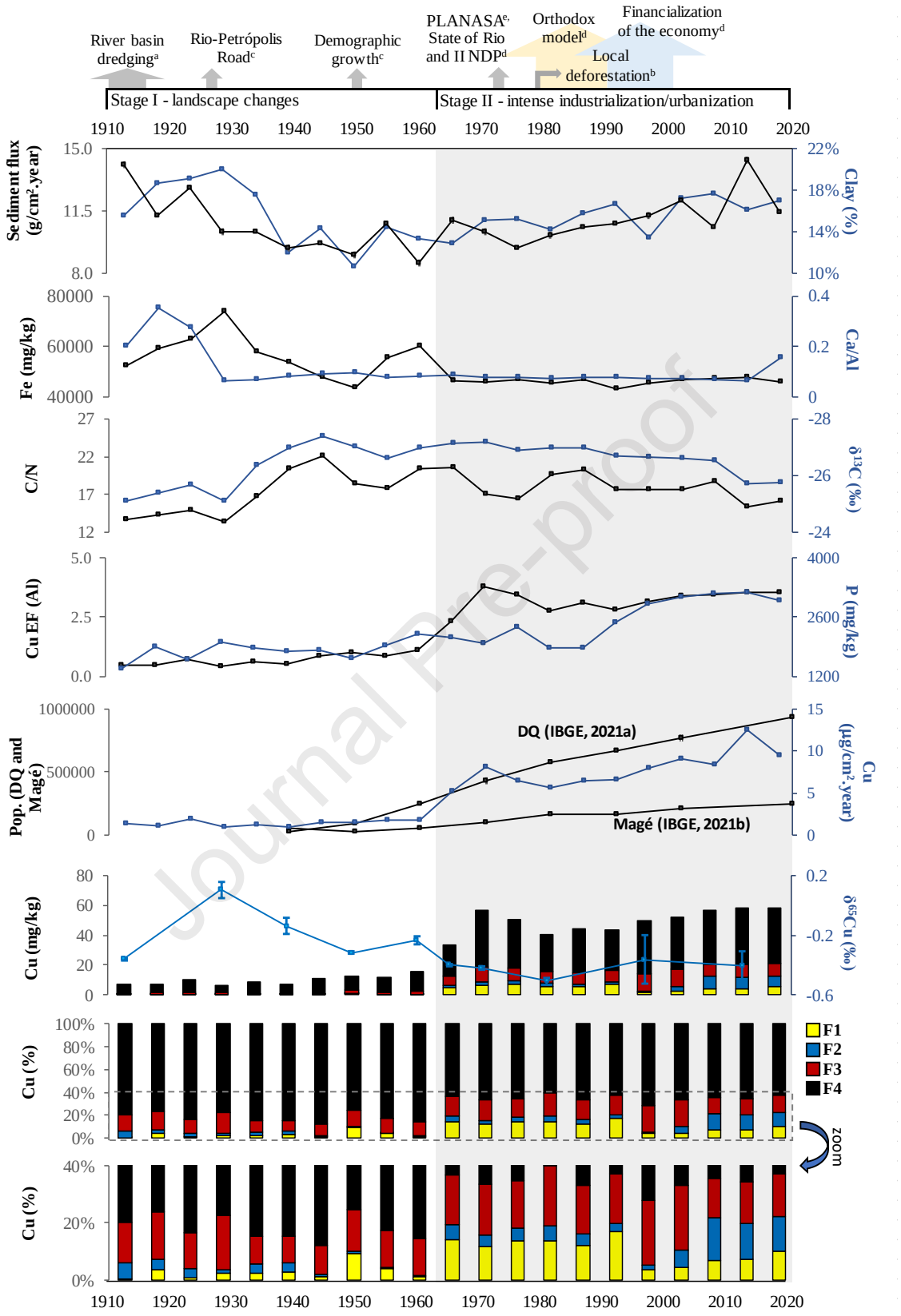

909
910 Figure 2 – Historical evolution of the main parameters. [a]Brito et al. (2019); [b]Borges et al. (2009);
911 [c]AGEVAP (2021); [d]de Oliveira & Rodrigues (2009); [e]Lima (2006).

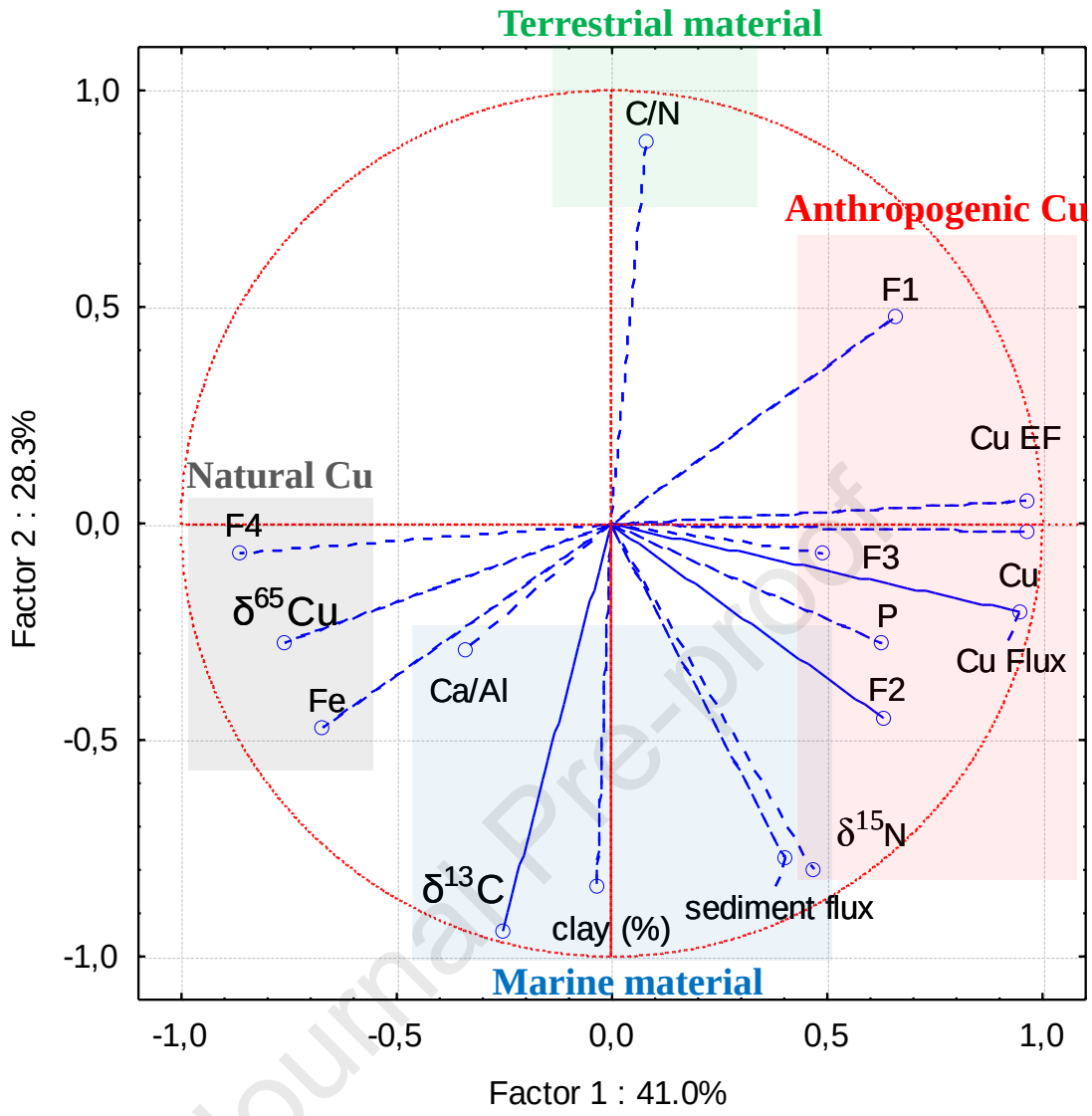

912

913 Figure 3.Principal Components Analyses (PCA) of the geochemical dataset.

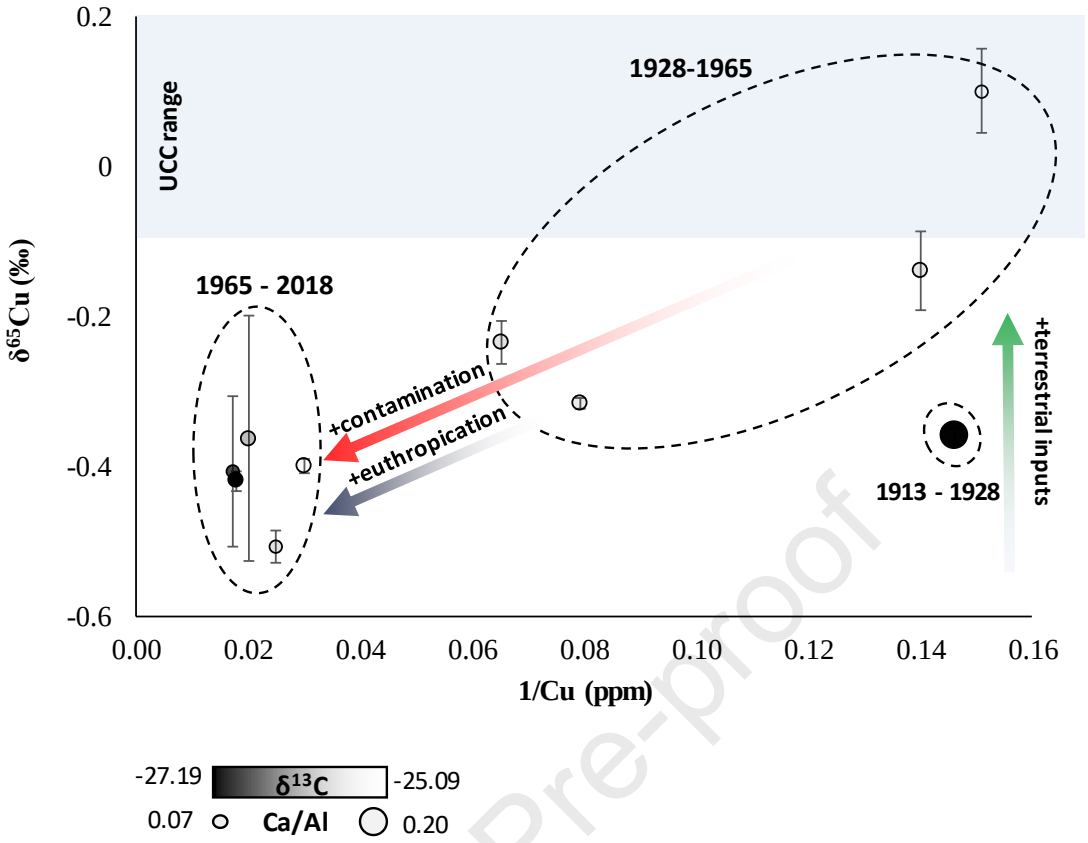

914

915

916 Figure 4 - $\delta^{65}Cu$ x 1/Cu (ppm). Gradients of grey refer to the range of $\delta^{13}C$ values, while gradients of size
917 refer to the range of Ca/Al values. The red arrow represents increasing anthropogenic contamination
918 between Stage I (after 1928) Stage II. Green arrow: "increased terrestrial inputs"; Red arrow: "increased
919 contamination"; Grey arrow: increased eutrophication". UCC – Upper Continental Crust (0.08±0.17%;
920 Vance et al., 2008; Takano et al., 2014; Thompson et al., 2014; Moynier et al., 2017).

921

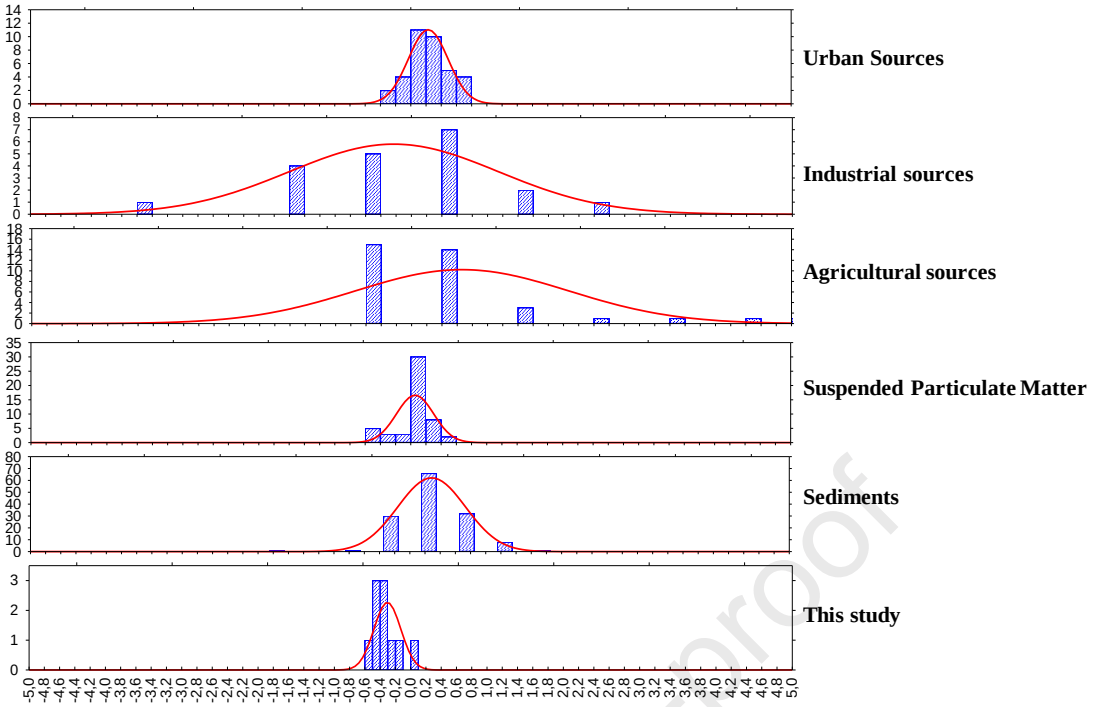

922

923 Figure 5 – δ^{65}Cu in this work and potential sources. δ^{65}Cu histograms in environmental matrices include
924 the expected normal. Y axis displays the number of observations. Sources: **Agricultural sources** (El Azzi
925 et al., 2013 ; Babicsanyi et al., 2014; 2016 ; Blotevogel et al., 2018), **Industrial sources** (Bigalke et al.,
926 2010 ; Novak et al., 2016; Viers et al., 2018; Xia et al., 2022) ; **Urban sources** (Dong et al., 2017 ; Souto-
927 Oliveira et al., 2018 ; 2019 ; Jeong et al., 2021a) ; **Sediments** (Petit et al., 2008; Thapalia et al., 2010; El
928 Azzi et al., 2013; Babcsányi et al., 2014; Little et al., 2017; Roebbert et al., 2018;; Ciscato et al., 2019 ;
929 Jeong et al., 2023).

930

931

Highlights

- Chronological survey of a well-constrained Brazilian mangrove core
- Cu isotopes respond to shifts from marine to geogenic dominance
- Sediments record the evolution of Cu fluxes along periods of urban and industrial development
- Mangrove sediments record anthropogenic Cu isotope fingerprint
- Anthropogenic inputs yielding increased bioavailability of Cu in mangrove sediments

Author statement

João Barreira - Conceptualization, Investigation, Methodology, Sampling, Formal analysis, Validation, Elaboration of Maps and Figures, Writing – original draft
Daniel F. Araújo - Conceptualization, Investigation, Methodology, Validation, Supervision, Writing – original draft
Breno Q. A. Rodrigues – Sampling, Formal analysis, Validation
Myller Tonhá - Methodology, Formal analysis, Validation
Rafael de Araújo - Formal analysis, Validation
Carlos Eduardo Souto de Oliveira - Methodology, Formal analysis, Validation
Marly Babinski - Methodology, Validation, Resources
Joël Knoery - Writing – original draft
Christian J. Sanders- Conceptualization, Formal analysis, Validation, Resources, Writing – original draft
Jérémie Garnier - Conceptualization, Investigation, Data curation, Validation, Resources, Supervision, Writing – original draft.
Wilson Machado- Conceptualization, Investigation, Sampling, Data curation, Validation, Writing – original draft, Funding acquisition, Project administration, Resources, Supervision

Declaration of interests

☒ The authors declare that they have no known competing financial interests or personal relationships that could have appeared to influence the work reported in this paper.

☐ The authors declare the following financial interests/personal relationships which may be considered as potential competing interests: